

## Evolutionary games defined at the network mesoscale: The Public Goods game

Jesús Gómez-Gardeñes,<sup>1,2,3,a)</sup> Miguel Romance,<sup>1</sup> Regino Criado,<sup>1</sup> Daniele Vilone,<sup>4</sup> and Angel Sánchez<sup>2,4,5</sup>

<sup>1</sup>*Departamento de Matemática Aplicada, Universidad Rey Juan Carlos, 28933 Móstoles, Madrid, Spain*

<sup>2</sup>*Institute for Biocomputation and Physics of Complex Systems (BIFI), Universidad de Zaragoza, 50018 Zaragoza, Spain*

<sup>3</sup>*Departamento de Física de la Materia Condensada, Universidad de Zaragoza, 50009 Zaragoza, Spain*

<sup>4</sup>*Grupo Interdisciplinar de Sistemas Complejos (GISC), Departamento de Matemáticas, Universidad Carlos III, 28911 Leganés, Madrid, Spain*

<sup>5</sup>*Instituto de Ciencias Matemáticas CSIC-UAM-UC3M-UCM, 28049 Cantoblanco, Madrid, Spain*

(Received 1 November 2010; accepted 13 December 2010; published online 29 March 2011)

The evolutionary dynamics of the Public Goods game addresses the emergence of cooperation within groups of individuals. However, the Public Goods game on large populations of interconnected individuals has been usually modeled without any knowledge about their group structure. In this paper, by focusing on collaboration networks, we show that it is possible to include the mesoscopic information about the structure of the real groups by means of a bipartite graph. We compare the results with the projected (coauthor) and the original bipartite graphs and show that cooperation is enhanced by the mesoscopic structure contained. We conclude by analyzing the influence of the size of the groups in the evolutionary success of cooperation. © 2011 American Institute of Physics. [doi:10.1063/1.3535579]

Evolutionary game dynamics on graphs has become a hot topic of research during the last years. The attention has been mainly focused on two-player games, such as the Prisoner's Dilemma game, since the pairwise interactions can be easily implemented on top of networked substrates. However, for  $m$ -player games, such as the Public Goods game, the microscopic description about the pairwise interactions contained in the network is not enough, since  $m$ -player game are intrinsically defined at the mesoscopic network level. This mesoscopic level describes how individuals engage into groups where the Public Goods games are played. However, the actual group structure of networks has not been considered in the literature, being automatically substituted by a fictitious one. In this work, we study the emergence of cooperation in collaboration networks, by incorporating the real group structure to the evolutionary dynamics of the Public Goods game. Our results are compared with those obtained when the mesoscopic structure is ignored. We show that cooperation is actually enhanced when the group structure is taken into account, thus providing a novel structural mechanism, relying on the mesoscale level of large social systems, that promotes cooperation. Moreover, we further show that the particular characteristics of the group structure strongly influence the survival of cooperation.

### I. INTRODUCTION

Evolutionary game theory on graphs is recently attracting a lot of interest among the community of physicists working

on complex systems.<sup>1,2</sup> This is a very appealing research topic because it combines two important ideas. First, interactions take place on a (possibly complex) network,<sup>3,4</sup> generalizing the lattice perspective; second, that the dynamics taking place on that substrate needs not be the traditional one, but rather it can arise from an evolutionary approach.<sup>5</sup> On the other hand, from the applications viewpoint, studying evolutionary games on graphs is one of the several avenues proposed to understand the emergence of cooperation in different contexts.<sup>6</sup> This is a most relevant issue that arises, for instance, in understanding the origin of multicellular organisms,<sup>7</sup> of altruistic behavior in humans and primates,<sup>8</sup> or the way advanced animal societies work,<sup>9,10</sup> to name a few.

Research on evolutionary game theory on graphs focused on the problem of the emergence of cooperation has considered mainly the Prisoner's Dilemma game (PDG).<sup>11,12</sup> The Prisoner's Dilemma game describes a situation in which cooperation is hampered by the players' temptation to defect (defecting yields more payoff than cooperating when facing a cooperator) and by the risk arising from cooperation (cooperating with a defector yields the lowest payoff).<sup>13</sup> This leads to a social dilemma because when players cooperate both the total benefit and the individual benefit are higher than when mutual defection occurs. While evolutionary dynamics leads all the individuals to defection when interactions take place in a well-mixed population (every player interacts with every other one), the existence of a network structuring the population can sometimes promote the emergence of cooperation,<sup>14</sup> but this depends strongly on the details of the network and the dynamics.<sup>2,15</sup>

Much less attention has been paid to the  $m$ -player generalization of the PDG, also called Public Goods Game (PGG)

<sup>a)</sup>Electronic mail: gardenes@gmail.com.

(Ref. 16): Cooperators contribute an amount  $c$  (“cost”) to the public good; defectors do not contribute. The total contribution is multiplied by an enhancement factor  $r < m$ , and the result is equally distributed between all  $m$  members of the group. Hence, defectors get the same benefit of cooperators at no cost, i.e., they free-ride on the cooperators’ effort. This is an alternative view of the social dilemma posed by the so-called tragedy of the commons.<sup>17</sup> As with the PDG, the evolutionary outcome of the PGG differs if played on a well-mixed population (where once again defection is selected) or on a network structure. Thus, Brandt *et al.*<sup>18</sup> showed that local interactions can promote cooperation in the sense that full cooperation is obtained for values of  $r$  well below the critical value  $r = m$ . This result, arising from simulation in a hexagonal lattice, was later generalized to other lattices in Ref. 19 and to scale-free graphs<sup>20</sup> in Ref. 21.

In this work, we focus on the mesoscopic structure of the networks and relate it to the situation represented by a PGG. Applications of this game arise naturally when a number of people have to work together toward a common goal, either to obtain some benefits or to avoid some negative effects. While trying to stabilize the Earth’s climate is a dramatic example of the latter,<sup>22</sup> coauthoring scientific papers is a direct application of the PGG in the positive sense. This provides a specific setting in which we can test the ideas about the emergence of cooperation in PGG on real social networks, as several collaboration networks have been mapped and are publicly available.<sup>23–25</sup> In this respect, it is worth noticing that the asymptotic behavior of evolutionary games in real social networks can be very different from that observed in model networks, and, in fact, mesoscopic scales, clustering, and motifs have been shown to play a key role in governing the game dynamics.<sup>26–29</sup> Therefore, it is important to assess to which degree, if at all, is cooperation promoted in PGG on collaboration networks. On the other hand, while collaboration networks are in fact bipartite, as coauthors are connected to papers, they are very often used in a projected mode, by connecting directly coauthors among themselves. Thus, the question arises as to the relevance of the mesoscopic structure (as defined by the papers) and the possible differences it may give rise to when the original bipartite or the projected network are considered. This is the sense in which the present work contributes to the advancement of our knowledge of the PGG on graphs, going beyond the results on model networks<sup>19,21</sup> to an analysis in depth of the effects of the group/mesoscopic features of real networks, which, to our knowledge, have never been studied in the context of PGG. On the other hand, as the group features of real collaboration networks can be easily captured by model bipartite graphs, our approach paves the way to a more careful study about the impact of the mesoscopic structural patterns on the evolutionary success of cooperation.

This paper is structured as follows: In Sec. II, we introduce the usual formulation of the PGG on complex networks and present the new formulation based on bipartite graphs, incorporating the interaction groups, i.e., the mesoscale structure of the population. Besides, in this section, we briefly introduce two different versions of the PGG and the different evolutionary rules we will use. In Sec. III, we focus

on scientific collaboration networks to show the different evolutionary outcomes of the projected and the bipartite representations. Namely, we show that the mesoscopic structure composed of the interaction groups plays a relevant role in the promotion of cooperation. In Sec. IV, we focus on the structural characteristics of the mesoscale. In particular, we analyze the role of the size of the interaction groups. The general conclusion of our analysis is that the larger the interaction groups, the more difficult is the cooperation promoted. Finally, in Sec. V, we summarize the main results and pose some relevant questions that arise from them.

## II. MODELING EVOLUTIONARY DYNAMICS OF PUBLIC GOODS GAME

### A. The evolutionary Public Goods game

The classical setting of a PGG models an economic or social group of  $m$  agents whose strategies can be cooperation (C) or defection (D). As explained above, if an agent cooperates, she invests a quantity  $c$  into the public pot whereas defectors do not contribute. Therefore, in a group with  $x$  cooperators (and  $m - x$  defectors), the total amount of investments is  $xc$ . This amount is then multiplied by an enhancement factor  $r > 1$  so that the total investment increases to  $rx$ . This amount is then distributed among all the participants of the PGG regardless of their contributions. Therefore, the benefit of each defector will be

$$f^D = \frac{rx}{m}, \quad (1)$$

while for a cooperator the benefit decreases to  $f^C = f^D - c$ . From these benefits, it is obvious that defectors will earn more than cooperators,  $f^D \geq f^C$ . Moreover, while  $f^D \geq 0$ , cooperators only have positive benefits when  $rx > m$ . This means that a lonely cooperator playing with a group of defectors will always lose ( $f^C < 0$ ) whenever  $r < m$ . Therefore, the Nash equilibrium of a PGG with  $r < m$  is a full defection situation (i.e., a group in which all players defect). However, this equilibrium is not Pareto optimal since full defection yields zero total reward whereas if everyone contributes to the PGG (full cooperation) the group will obtain the maximum total reward. Thus, here is where the social dilemma lies.

In an evolutionary context, individuals are not considered fully rational, so that they do not necessarily play a Nash equilibrium found from a rational analysis of the PGG. Besides, agents are not organized into a single group but in general a large population of  $N \gg m$  agents is allowed to organize into a large number of groups with  $m$  agents. The relevant difference with the classical setting is the introduction of a dynamical evolution: Agents play the game several times, and they are allowed to change their strategy after each round of the game. These strategy changes obey certain evolutionary rules by which agents evaluate their performance comparing their fitness with those of the rest of the population (see Sec. II D).

In a well-mixed population, the agents play within several groups during the different rounds of the game. In

particular, before each round of the PGG, the groups are formed randomly. Under this well-mixing assumption, it can be shown that the evolutionary dynamics ends up in full defection whenever  $r < m$ . Therefore, defection again dominates over cooperation as in the (static) classical setting. Driven by the abundance of examples in which cooperation is observed in social, economical, and biological situations similar to those defined by the PGG, it is clear that some mechanisms beyond irrationality and evolution are at the core of the survival of cooperation. In this line, several mechanisms have been proposed such as the influence of human beliefs,<sup>30–32</sup> the addition of costly punishment,<sup>18,33</sup> meaning the possibility of punishing defectors after a round of the PGG, or the addition of reputation<sup>18</sup> to agents, which signals the behavior of these players in past rounds of the game. These social-based mechanisms allow to enhance the contributions to the PGG, thus favoring the survival of cooperative behaviors.

## B. The Public Goods game on complex networks

The aforementioned mechanisms (punishment and reputation) are clearly based on human behaviors that are plausible to appear in social systems. However, cooperation in the PGG can also be promoted by taking into consideration the structure of interaction between players. To this aim, one leaves out the well-mixing assumption and works with a static substrate of interactions. As introduced above, in Ref. 18, it was shown that, in the case of the PGG, cooperation was significantly promoted when considering Euclidean lattices. The importance of the structure of interactions in the success of cooperation in the general context of evolutionary game theory is underlined by the term *network reciprocity*.<sup>6</sup>

The interaction backbone of real social systems is however far from Euclidean structures. In particular, many studies in the last decade have addressed the characterization of such social systems as complex networks.<sup>3,4</sup> These networks are a collection of  $N$  nodes (accounting for each agent of the system) and  $L$  links (describing the interaction between pairs of agents). Complex networks typically display structural patterns that are absent in regular geometries, such as the small-world property<sup>34</sup> or scale-free patterns for the number of connections of the agents.<sup>20</sup> On the other hand, real complex networks are sparse ( $L \sim N$ ) meaning that the well-mixed assumption (which would imply that  $L \sim N^2$ ) does not hold. Thus, it is necessary to study how the structure of these networks affects the evolution of cooperation. As in the case of regular lattices, the first evolutionary social dilemma to be studied on top of networks was the PDG. The main result of these studies is that, under certain conditions,<sup>2,15</sup> cooperation is further enhanced with respect to the case of regular lattices. Moreover, it was observed that the degree-heterogeneity of scale-free networks significantly increases the survival of cooperation with respect to random complex networks,<sup>35–37</sup> as was subsequently shown<sup>21</sup> for PGG, thus reinforcing the message that scale-free structures are natural promoters of cooperation.

The implementation of the PGG on top of complex networks is, however, not as straightforward as in the case of

the PDG. The reason is clear: While the PDG is defined for pairwise interactions and thus the possible games are dictated by the collection of links of the network, for  $m$ -player groups ( $m > 2$ ), we do not have the information about how to engage players in groups. Therefore, some *a priori* assumptions about the inner group structure of complex networks have to be made. In particular, most of the works in the literature about the PGG on networks<sup>21,38–46</sup> overcome this lack of information about their group structure, by assuming that a complex network automatically defines  $N$  different groups of players. Namely, each of these groups is defined by considering one agent  $i$  and her  $k_i$  neighbors as dictated by the network topology (see Fig. 1). Obviously, the size of these groups is not regular since the number of neighbors each agent has can fluctuate around the average connectivity of the complex network. In scale-free networks, these fluctuations diverge since the probability of finding an individual with  $k$  neighbors follows a power-law,  $P(k) \sim k^{-\gamma}$  with  $2 \leq \gamma \leq 3$ . Thus, one finds a large number of small size groups (those centered around agents with small connectivity) and a few of them composed of many agents (corresponding to groups formed around the hubs of the system). On the other hand, since each individual  $i$  participates in  $k + 1$  groups, the hubs participate in a large number of groups.

Given the above definition for the group structure, the implementation of the evolutionary PGG is as follows. At each time step of the evolutionary dynamics, each player  $i$  plays the PGG within the  $k_i + 1$  groups she belongs to (using the same strategy in each PGG). Once all the games are played, each agent  $i$  collects the total benefit,  $f_i$ , obtained. If the agent plays as a cooperator, she pays a cost,  $c_i$ , for participating in each of the  $k_i + 1$  groups. Here we will consider two situations for assigning the value of the investment made in each of the PGG she participates (as introduced in Ref. 21). First, we consider that a cooperator agent pays a fixed cost  $c_i = z$  per game (FCG) played; thus, her total investment raises to  $(k_i + 1)z$ . The second option is to assume a fixed cost  $z$  per individual (FCI) playing as cooperator.

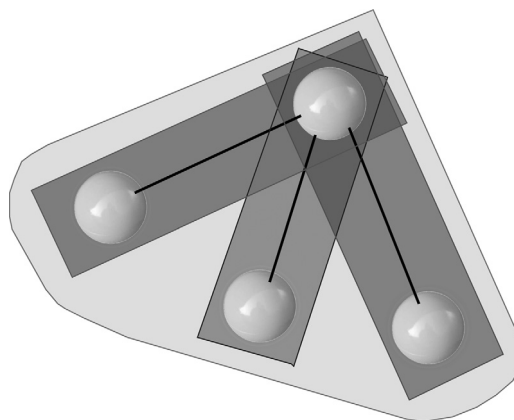


FIG. 1. Schematic representation of the usual way for defining the interaction groups of the PGG on complex networks. Each of the four agents defines a group composed of her and its neighbors. As a result, the above graph contains three groups composed of two nodes and a big one containing the four nodes of the graph.

Therefore, in this latter scenario, the quantity  $z$  is equally distributed by contributing a quantity  $c_i = z / (k_i + 1)$  to each group she participates. The convenience of using either the FCG setting or the FCI one depends on the particular scenario of the PGG. For instance, the FCG setting deals with accumulative costs, such as the taxes associated to each financial activity. On the other hand, the FCI setting addresses situations in which the cost is associated with a finite resource equally distributed among individuals, such as the available time to distribute among parallel tasks.

Having in mind the above two settings for deciding the contributions of cooperator players, we can write the benefits of each agent given her strategy and those of her first and second neighbors. If we denote by  $x_i^t$  the strategy of agent  $i$  during round  $t$  of the PGG, so that  $x_i^t = 1$  when playing as cooperator and  $x_i^t = 0$  if defecting, the benefit  $f_i(t)$  obtained after the round reads

$$f_i(t) = \sum_j 1^N A_{ij} \frac{r \left( \sum_{l=1}^N A_{jl} x_l^t c_l + x_j^t c_j \right)}{k_j + 1} - k_i x_i^t c_i + \frac{r \left( \sum_{j=1}^N A_{ij} x_j^t c_j + x_i^t c_i \right)}{k_i + 1} - x_i^t c_i. \quad (2)$$

In the above equation, we have made use of the adjacency matrix of network whose entries are  $A_{ij} = A_{ji} = 1$  when  $i$  and  $j$  are connected and  $A_{ij} = 0$  otherwise, with  $A_{ii} = 0$  (no self-links). Note that the first two terms of Eq. (2) correspond to the PGG played within the groups formed around the neighbors of  $i$  while the last two terms account for the game played by  $i$  and her neighbors.

### C. The Public Goods game on bipartite graphs

The definition of the groups where the PGG takes place as the sets formed by each agent and her network neighbors arises from using the network of contacts as the map of agent interactions. However, most social networks are constructed from real data containing information about the groups formed by individuals. The well-known examples are collaboration networks in which agents can be scientists collaborating to perform research.<sup>23–25</sup> In Fig. 2, we plot how collaboration data are usually collected to form a projected (or one-mode) complex network of the interactions among

agents (the coauthor network). The central plot corresponds to the original data containing several collaboration groups among six agents. These groups are then translated into a complex network by projecting the original data (left plot). The collection of groups then transforms into a starlike graph in which there is a central hub (node 6) with five neighbors, some of them connected and thus forming triangles with the central hub. One easily realizes that groups defined on the projected network itself (following the definition given in Sec. II B) are rather different from the original ones.

On the other hand, one can take advantage of the information available in collaboration data by constructing a bipartite graph.<sup>47–49</sup> The structure of this bipartite graph is represented in the right plot of Fig. 2. As observed, the bipartite representation contains two types of nodes denoting agents (left column of round nodes) and collaborations (right column of squared nodes), respectively. It is clear that connections are restricted to link nodes of different types (i.e., belonging to different columns). Thus, such a bipartite representation preserves the information about the group structure of the original data and constitutes a well-suited framework for studying dynamical processes intrinsically defined at a system mesoscale<sup>50</sup> (in our case defined by the collaboration groups) as is the case of the PGG.

Let us now formalize the bipartite graph in which the evolutionary dynamics of the PGG takes place. The graph will be composed of  $N$  agents playing the PGG within  $P$  groups. The particular way agents engage into groups will be encoded by a  $P \times N$  matrix  $B_{ij}$  usually called biadjacency matrix. Given the bipartite structure of the graph, the  $i$ -th row accounts for the individuals participating in group  $i$ , so that agent  $j$  is engaged in group  $i$  whenever  $B_{ij} = 1$  while  $B_{ij} = 0$  when she is absent (note that now  $B_{ii}$  needs not be zero as rows and columns represent different entities). Alternatively, the  $i$ -th column contains the information about the groups containing agent  $i$ :  $B_{ji} = 1$  when agent  $i$  participates in group  $j$  and  $B_{ji} = 0$  otherwise. Given the biadjacency matrix we can calculate the number of groups agent  $i$  takes part,  $q_i$ , as

$$q_i = \sum_{j=1}^P B_{ji}, \quad (i = 1, \dots, N). \quad (3)$$

Alternatively, the number of participants contained in group  $i$ ,  $m_i$ , reads

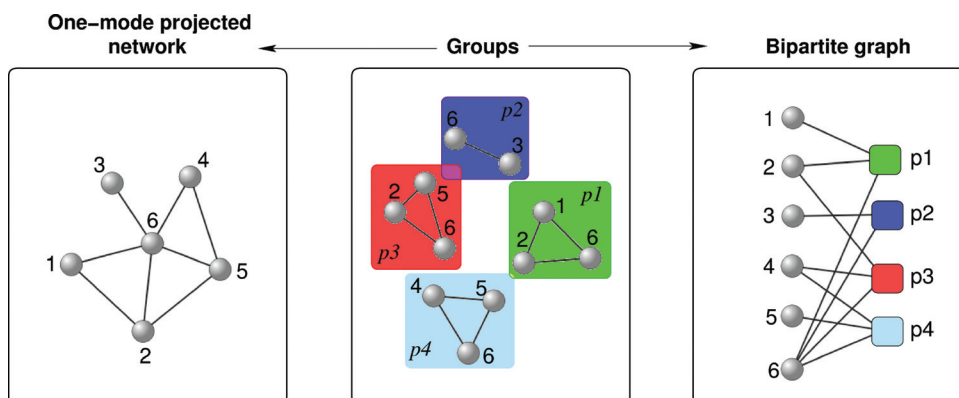


FIG. 2. (Color online) Schematic representation of the two different forms of encoding collaboration data. In the central plot several collaboration groups represent the original data. The interactions among agents can be translated into a projected complex network (left). However, if one aims at preserving all the information about the group structure, a representation as a bipartite graph (right) is more appropriate.

$$m_i = \sum_{j=1}^N B_{ij}, \quad (i = 1, \dots, P). \quad (4)$$

Having introduced the structure of the bipartite graph describing the relations between agents and groups, we model the PGG. At each time step, each player  $i$  ( $i = 1, \dots, N$ ) plays a round of the PGG each at every group she participates in as defined by the biadjacency matrix of the bipartite graph,  $B_{ji} = 1$  ( $j = 1, \dots, P$ ). Obviously, the benefit obtained by the agent depends on both her strategy and those of the agents participating in the same groups. The net benefit after playing round  $t$  of the PGG now reads

$$f_i(t) = \sum_{j=1}^P \frac{rB_{ji}}{m_j} \left[ \sum_{l=1}^N B_{jl}x_l^t c_l \right] - x_i^t c_i q_i \quad (5)$$

Note that the sum in the above expression accounts for  $q_i$  PGGs played by  $i$  while the last term is for the cost associated to participating as cooperator.

### D. Strategy update: Evolutionary dynamics

After a round of the PGG is played, agents update their strategies. This update is driven by the benefits obtained by the agent and her neighbors in the last round of the game. Thus, the update stage keeps the local character by restricting the information available to agents about the benefits of other players to their local (one-mode) network neighborhoods. Note that the group structure described in the bipartite representation plays no role in this stage, as update rules make use of the network of contacts. Thus, the update process takes place in the same way regardless of the representation (one-mode network or bipartite graph) of the PGG we are using.

In this work, we will use three different update rules in order to test the robustness of the results obtained. In all the update rules, each agent decides to use the strategy of a given neighbor  $j$  in the next round of the game ( $x_i^{t+1} = x_j^t$ ) or to stay the same ( $x_i^{t+1} = x_i^t$ ). The three update rules work as follows:

- Unconditional Imitation (UI):<sup>14</sup> agent  $i$  compares her payoff with her neighbor with the largest payoff, say agent  $j$ . Agent  $i$  will copy the strategy of agent  $j$  provided  $f_i < f_j$ . Otherwise, agent  $i$  will remain unchanged. The probability of copying agent  $j$  is given by

$$P_j = \Theta(f_j - f_i) \text{ with } f_j = \max\{f_l | A_{il} = 1\}, \quad (6)$$

where  $\Theta(x)$  is the Heaviside step function,  $\Theta(x) = 1$  when  $x > 0$  and  $\Theta(x) = 0$  for  $x \leq 0$ .

- Fermi rule:<sup>51,52</sup> agent  $i$  chooses one neighbor at random, say agent  $j$ , and compares their respective benefits. The probability that  $i$  copies the strategy of the chosen neighbor obeys a saturated Fermi function of the benefit difference  $f_i - f_j$ . Thus, the probability that  $i$  decides to take the strategy of an agent  $j$  reads

$$P_j = \frac{A_{ij}}{k_i} \cdot \frac{1}{1 + e^{\beta(f_i - f_j)}}. \quad (7)$$

where  $\beta$  is a free parameter of the model.

- Moran rule (MOR):<sup>15,53</sup> agent  $i$  chooses one of her neighbors proportionally to her payoff. Subsequently, agent  $i$  adopts automatically the state of the chosen neighbor. Therefore, the probability of choosing agent  $j$  is given by

$$P_j = \frac{A_{ij}f_j}{\sum_{l=1}^N A_{il}f_l}. \quad (8)$$

These three update rules contain different evolutionary ingredients. In particular, UI and MOR use global knowledge about the benefits of the neighbors since they evaluate all of them. On the contrary, the Fermi update chooses one neighbor randomly. Concerning the stochastic character of the agent's decisions, we note that both Fermi (for small and moderate values of  $\beta$ ) and MOR updates are purely stochastic and they even allow mistakes, i.e., it is possible to copy the strategy of a neighbor with smaller benefit. In contrast, UI is purely deterministic and errors are not admitted. Note that when  $\beta \gg 1$  (strong selection limit) the saturated Fermi function turns into a Heaviside step function thus mimicking the behavior of UI. However, the differences in the degree of knowledge about neighbors of both setting persist. In the following, we will use  $\beta = 1$  for the Fermi update since the results are quite robust around this value.

### III. COOPERATION IN SCIENTIFIC COLLABORATIONS: PROJECTED VERSUS BIPARTITE NETWORKS

In this section, we implement the PGG on top of a real collaboration network. The network is composed by  $N = 13861$  scientists and the collaboration data are obtained from  $P = 19465$  papers appeared in the *cond-mat* section of the arXiv preprint server.<sup>23</sup> This collection of papers is obtained after computing the giant connected component of the (projected) coauthor network of the original data set that has 16726 authors and 22015 papers. In Fig. 3, we plot the degree distribution of the coauthor network and those of the bipartite (authors–papers) graph. Both the probability of finding one author with  $k$  coauthors,  $P(k)$ , and that of having an author collaborating in  $q$  papers,  $P(q)$ , have broad profiles. On the other hand, the probability that a paper is coauthored by  $m$  researchers,  $P(m)$ , shows an exponential decay. This homogeneous distribution for the number of authors coauthoring one paper is a very important difference arising when comparing the (one-mode) coauthor network with the bipartite representation of the collaboration data.

The structural differences between the coauthor network and the bipartite graph imply that the dynamical processes implemented on top of them can yield different results. In particular, modeling the PGG without any knowledge of the real group structure will give as a result the definition of large groups centered around hubs of the coauthor network [see Fig. 3(a)]. However, this definition strongly contrasts with the homogeneous distribution  $P(m)$  for the number of authors collaborating in one paper. Thus, we will compare the outcome of the PGG evolutionary dynamics using the one-mode coauthor network, as originally proposed by

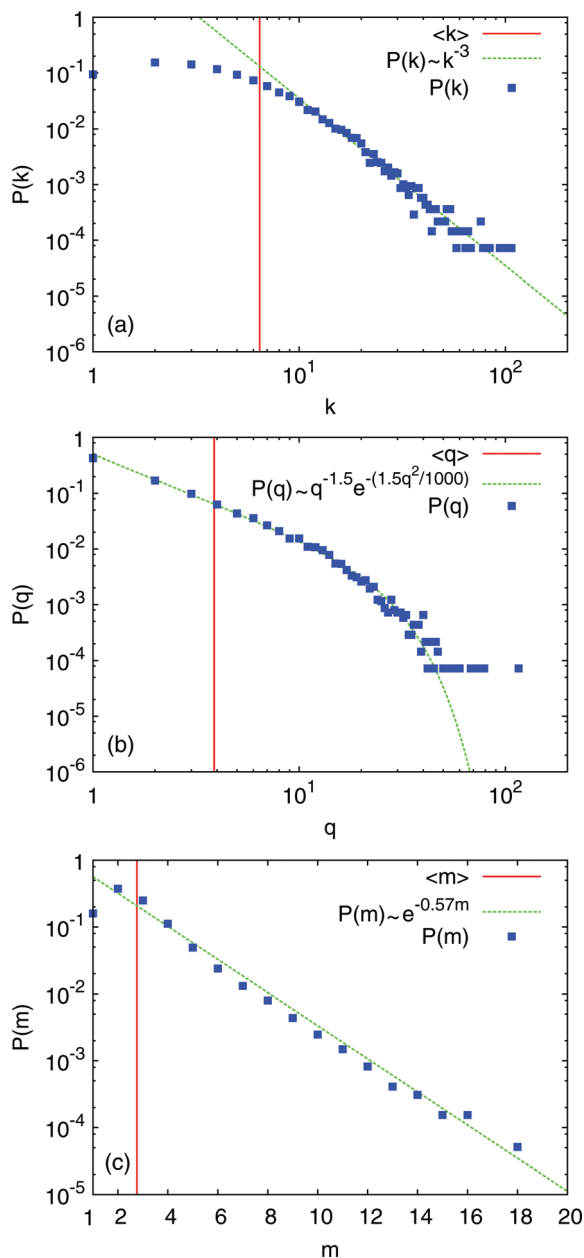


FIG. 3. (Color online) Structural analysis of the *cond-mat* scientific collaboration network. In (a), we plot the degree distribution,  $P(k)$ , of the projected (one-mode) network (coauthor network). This distribution displays a long tail decaying as  $P(k) \sim k^{-3}$ . The average connectivity is  $\langle k \rangle = 6.44$  as indicated (in this and subsequent plots) by a red vertical line. Plots (b) and (c) show the connectivity patterns of the associated bipartite graph. In (b), we show the degree distribution of authors,  $P(q)$ , i.e., the probability of finding an author contributing to  $q$  papers. The behavior of this distribution denotes a sharp decay, thus indicating that the initial power-law behavior truncates for large  $q$  and, as indicated in the plot, the distribution behaves as  $P(q) \sim q^{-1.5} e^{-1.5q^2/10^3}$ . The average number of papers per author is  $\langle q \rangle = 3.87$ . On the contrary, in (c), we plot the probability that a paper is coauthored by  $m$  authors,  $P(m)$ . In this case,  $P(m)$  decays exponentially (note normal scale on  $x$  axis) as  $P(m) \sim e^{-0.57m}$ , so that, on average, papers are coauthored by  $\langle m \rangle = 2.76$  researchers.

Santos *et al.* in Ref. 21 and subsequently widely used in the works on the subject, with our new results obtained by working with the real collaboration data, i.e., with the bipartite graph, in which the group structure arises in a natural manner as defined by the set of papers.

We will focus on the evolution of the asymptotic value of the cooperation level,  $\langle c \rangle$ , as a function of the enhancement factor  $r$ . The cooperation level usually represents the fraction of the  $N$  individuals that cooperate in the stationary regime. Thus, in our simulations, we start by assigning randomly the initial strategies of the players,  $\{x_i^0\}$ , so that half of the population plays initially as cooperators and the other one as defectors. Then, we let the evolutionary dynamics evolve for  $\tau = 10^5$  rounds of the PGG and measure the stationary value of the cooperation level during  $T = 10^4$  additional rounds. Thus, the final value of  $\langle c \rangle$  is computed as

$$\langle c \rangle = \frac{1}{T \cdot N} \left( \sum_{t=\tau+1}^{\tau+T} \sum_{i=1}^N x_i^t \right). \quad (9)$$

The above definition of  $\langle c \rangle$  assumes that the evolutionary dynamics ends up in a dynamical equilibrium in which cooperators and defectors coexist. However, for the Fermi and MOR updates, depending on the precise values of  $r$ , this is not the case. Quite on the contrary, each run of the evolutionary dynamics for the same value of  $r$  (corresponding to a different set of initial conditions) ends up into either full defection or full cooperation. The strong stochasticity of the evolutionary dynamics, produced by the Fermi and MOR updates rules, drives the system evolution into one of those two absorbing states. Therefore, it is mandatory to perform a large number (at least  $10^3$  in our case) of different realizations (corresponding to different initial conditions) of the evolutionary dynamics. Obviously, in those cases, where the dynamical evolution always finishes in one of the two absorbing states, the reported value of  $\langle c \rangle$  is defined as the fraction of realizations in which the dynamics ends up in full cooperation.

Figure 4 shows the function  $\langle c \rangle(r)$  for both the (one-mode) coauthor network and the bipartite graph in six different scenarios. Namely, plots 4(a)–4(c) show the results for the PGG played with FCG, while in plots 4(d)–4(f), we show the case of the PGG played with FCI. As introduced in Sec. II D, for both the FCG and FCI versions of the PGG, we show the outcomes of the evolutionary dynamics when three update dynamics are at work. Namely, in plots 4(a) and 4(d), we use the MOR (strongly stochastic and using global knowledge) scheme, in plots 4(b) and 4(e) the Fermi rule (slightly stochastic and with limited knowledge), and finally, plots 4(c) and 4(f) correspond to UI update (purely deterministic and using global knowledge).

As can be seen from the plots, the average level of cooperation  $\langle c \rangle$  increases from  $\langle c \rangle = 0$  to  $\langle c \rangle = 1$  when the value of  $r$  exceeds some threshold  $r_c$ . The precise value of this threshold and the velocity of this transition depend strongly on the particular dynamical rule and the substrate of interactions used. It is clear that our main interest here is to confront the results of the PGG obtained using the one-mode network and the bipartite graph. The plots corresponding to the PGG with FCG clearly show that the cooperation level is always larger (meaning that it sets on for lower values of  $r$  and increases faster) when the structure of groups is that of the real collaboration data, i.e., of the bipartite representation. It

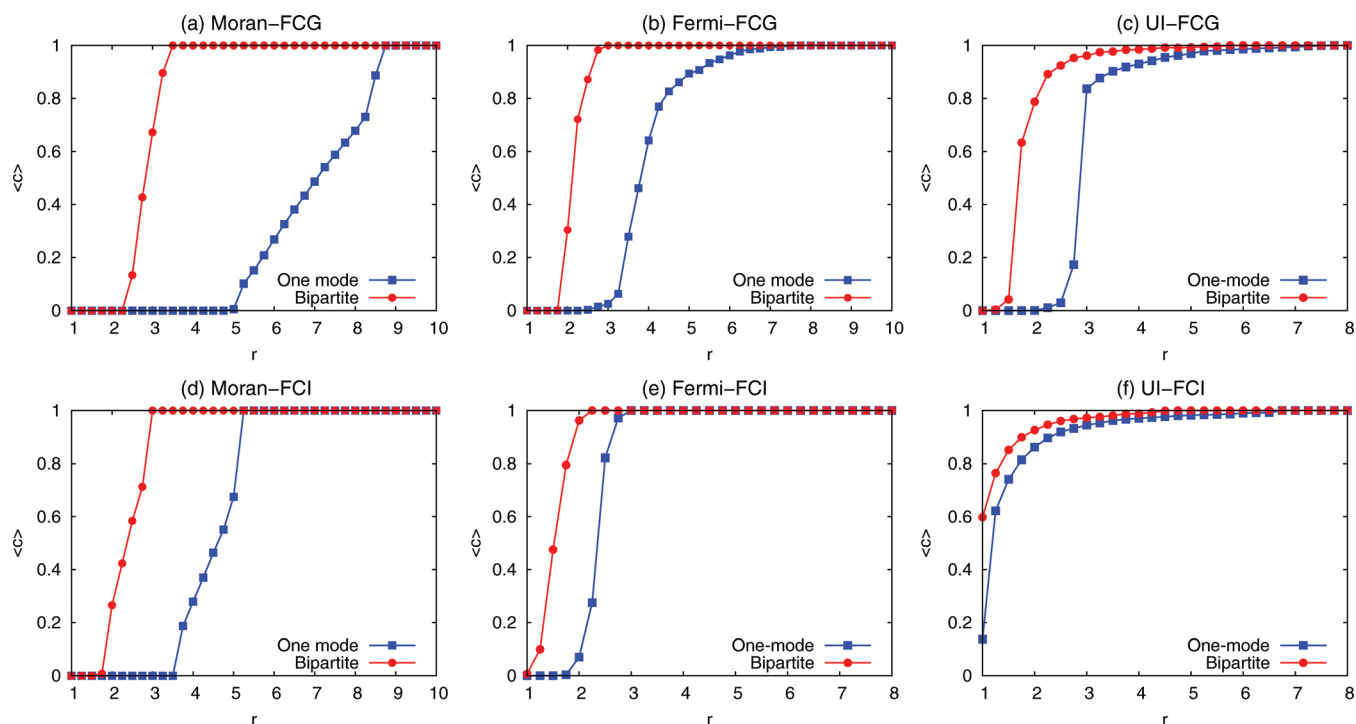


FIG. 4. (Color online) Cooperation level  $\langle c \rangle$  as a function of the enhancement factor  $r$  for the PGG played on top of the one-mode (projected) coauthor network and the bipartite graph preserving the original group structure. The first three plots (a), (b), and (c) correspond to the PGG with FCG, while the plots (d), (e), and (f) account for the PGG with FCI. For each of the two versions of the PGG, we show the evolution of the curves  $\langle c \rangle(r)$  for three different update rules: (a) and (d) MOR update, (b) and (e) Fermi rule, and (c) and (f) UI.

is also clear that the MOR update rule [plot 4(a)] gives rise to larger differences between the two substrates. Interestingly, we observe that the curve  $\langle c \rangle(r)$  corresponding to the bipartite graph is much more stable under update rule changes than its one-mode counterpart. On the other hand, for both the one-mode and the bipartite substrates, the onset of cooperation delays progressively as the stochastic character of the update rule increases, i.e., going from UI to the Fermi rule and from the Fermi rule to the MOR update.

As discussed above, the FCI setting is the most appropriate version of the PGG to model a scenario in which the resource associated to the cost is finite, and it is equally distributed among players. This ingredient applies in the case of scientific collaborations. The reason is clear, researchers have a limited amount of time/resources to invest in collaborating and it has to be partitioned among all the collaborations they share. In general, researchers participating in a large number of projects tend to contribute less (in terms of time and lab work) to each paper in which they appear. On the other hand, those researchers involved in a few collaborations tend to assume the largest part of the work to do. In the plots of Fig. 4 corresponding to the PGG in its FCI version, we find the same result as for the PGG with FCG: the group structure (contained in the bipartite graph) promotes cooperation. Again, the differences between both substrates are larger when using the MOR update while the stochasticity of the update rules delays the onset of cooperation in both cases.

Our findings yield several main conclusions about the role played by the mesoscale in the promotion of cooperation. The most important conclusion is that by considering

the real group structure, i.e., playing the PGG within the bipartite representation, we obtain a larger degree of cooperation than in the case of the PGG played in the projected network. This result is robust under variations of the PGG formulation and the update dynamics at work. The roots for such an enhancement of the cooperation are actually found on the small and homogeneous group sizes [see  $P(m)$  in Fig. 3] of the groups in which the PGG is played. Note, also in Fig. 3, that this homogeneous distribution for the size of the groups,  $P(m)$ , is combined with an heterogeneous one for the number of groups in which an agent engages,  $P(q)$ . This combination allow the existence of a significant number of players with large payoffs (those with large values of  $q$ ) while the groups are small enough for being far from a well-mixed situation. This is not the case for the PGG played in the usual way,<sup>21</sup> i.e., in the one-mode projected network, since the degree distribution  $P(k)$  automatically constrains the existence of a significant number of players participating in a large number of groups with the existence of the same quantity of large groups, in which cooperation is less favored.

Finally, the mesoscale properties contained in the bipartite graph also have important consequences for a well-known effect:<sup>21</sup> the promotion of cooperation when passing from the PGG with FCG to the PGG with FCI. As noted in Ref. 21, the increase in the degree of cooperation when playing with FCI has to do with the enhancement (with respect to the FCG case) of the payoff obtained by those nodes participating in a large amount of groups (i.e., those players having a large degree  $k$  in the one-mode projected network). For the bipartite representation, this payoff enhancement also applies

to those players having a large  $q$  when playing within the bipartite representation. Thus, the increase of cooperation when playing the PGG with FCI in both representations relies in the two long-tailed distributions for  $P(k)$  and  $P(q)$  as shown in Fig. 3. On the other hand, this boost of the cooperation is more apparent when dealing with the projected network setting than in the bipartite case. The reason for this different behavior is rooted in the distributions  $P(k)$  and  $P(q)$ . In the projected network each node of degree  $k$  participates in  $k + 1$  groups. Thus, even for those nodes with  $k = 1$ , the transition from the FCG setting to the FCI represent a change in their contribution. However, in the bipartite representation, the individuals are engaged in  $q$  groups. Thus, those individuals with  $q = 1$  do not change their contribution when passing from FCG to FCI. Moreover, from Fig. 3, we observed a large number of individuals sharing only one collaboration in the bipartite representation (more than the 40% of the population) in contrast to the smaller amount of leaves (less than the 10% of the nodes) in the one-mode network. These differences again confirm that the structural patterns encoded in the mesoscale of the network play a key role in the evolutionary success of the cooperation.

#### IV. INFLUENCE OF GROUP SIZE IN THE PROMOTION OF COOPERATION

Having shown that the mesoscopic group structure of collaboration networks strongly affects the promotion of cooperation, we now abandon the projected representation and focus on the bipartite one. In particular, we will address the issue of the influence of the size of the groups in the evolutionary dynamics of the PGG. To this end, and inspired in the model introduced by Ramasco *et al.*,<sup>47</sup> we propose the following way for constructing synthetic collaboration graphs. We start with an initial core of  $m$  nodes that defines the first group of our bipartite graph. At each time step of the growth process we add a new element that will define a new group of size  $m$ . To do this, the newcomer chooses one of the nodes already present in the graph. The probability  $P_i$  that a node  $i$  receives the link from a newcomer is proportional to the number of groups it belongs to,  $g_i$ ,

$$P_i = \frac{g_i}{\sum_j g_j}. \quad (10)$$

Once the newcomer has chosen the first node, say with node  $j$ , it closes the group by choosing other  $(m - 2)$  nodes randomly from the neighbors of  $j$ , i.e., among those nodes that participate in one or more groups with  $j$ . The above process is iterated until the graph contains  $N$  nodes (and  $N - m + 1$  groups). The above model, being extremely simple, allows to reproduce two main structural features observed in collaboration networks: the scale-free distribution for the number of contacts each individual has in the projected (coauthor) network and the nearly constant value for the number of authors appearing in a paper. In fact, this latter feature is used as a tunable parameter,  $m$ , in our network model, allowing us to explore the effect that this size has on the evolution

of cooperation. In the following, we will fix the size of the network to  $N = 5000$ , and we will work with  $m = 3, 5$ , and  $7$ .

Following the same strategy as in the previous section, we will compare the outcome of the evolutionary dynamics making use of three update rules (MOR, Fermi, and UI), and we will also analyze the PGG in both its FCG and FCI versions. In Fig. 5, we show the six plots corresponding to these scenarios. The initial setup and the numerical procedure are identical to those used in the previous section. The only novelty is the use of the rescaled enhancement factor,  $r' = r/m$ , so to compare the outcome of the PGG dynamics in different network topologies (they depend heavily on  $m$ )<sup>21,38</sup> here labeled by the group size  $m$ .

Let us start by analyzing the case of the PGG played with FCG. In this case, the curves  $\langle c \rangle(r/m)$  in plots 5(a) and 5(b), corresponding to the MOR and Fermi (stochastic) updates, behave as expected: Cooperation dominates for  $r/m > 1$  (i.e., when the enhancement factor is larger than the group size) while for  $r/m < 1$  it decays fast toward full defection. The decay becomes sharper as  $m$  increases so that we conclude that small groups benefit cooperation. The case of UI [plot 5(c)] confirms this conclusion about the negative effects of large groups. However, in this case, the curves  $\langle c \rangle(r/m)$  for  $m = 5$  and  $7$  point out a dramatic scenario for the survival of cooperation. While for the rest of the curves  $r/m = 1$  represent the point beyond which full cooperation dominates in those curves corresponding to UI with  $m = 5$  and  $m = 7$  the transition is very slow. Therefore, the effects of enlarging the group size in the mesoscopic structure of collaboration networks seem to have negative effects over cooperation, especially in the case when UI is the update mechanism at work.

Now we turn our attention to the PGG played with FCI. As before, we first focus on the stochastic update rules (MOR and Fermi). In the corresponding plots [5(d) and 5(e)], we observe that, for the same value of the group size  $m$ , cooperation is significantly enhanced with respect to the case of the PGG with FCG. In the case of the MOR update we also observe again (as in the PGG with FCG) that by increasing the group size the cooperation level decreases. However, for the Fermi rule, this is not the case (at variance with the PGG with FCG) and the curves  $\langle c \rangle(r/m)$  collapse in the transition region, placed around  $r/m \simeq 0.2$ . The case of the UI turns to be the most intriguing as in the PGG with FCG. However, in the case of the FCI version, the effects of enlarging the size of the groups have worse consequences as observed from the plot 5(f). As expected, for a group size of  $m = 3$  cooperation is enhanced with respect to the FCG situation; however, for  $m = 5$  and  $m = 7$ , both curves are nearly the same, and the situation is completely different to that observed for  $m = 3$ . First, for low values of  $r/m$ , the cooperation levels observed for  $m = 5, 7$  are rather large compared to the case  $m = 3$  and the other curves corresponding to different update rules. This sudden onset of cooperation is however followed by an extremely slow increase of the cooperation level. We have checked the roots of this behavior by looking at the dynamical evolution of the fraction of cooperators for several realizations of the dynamics. The result is that, despite the deterministic character of UI



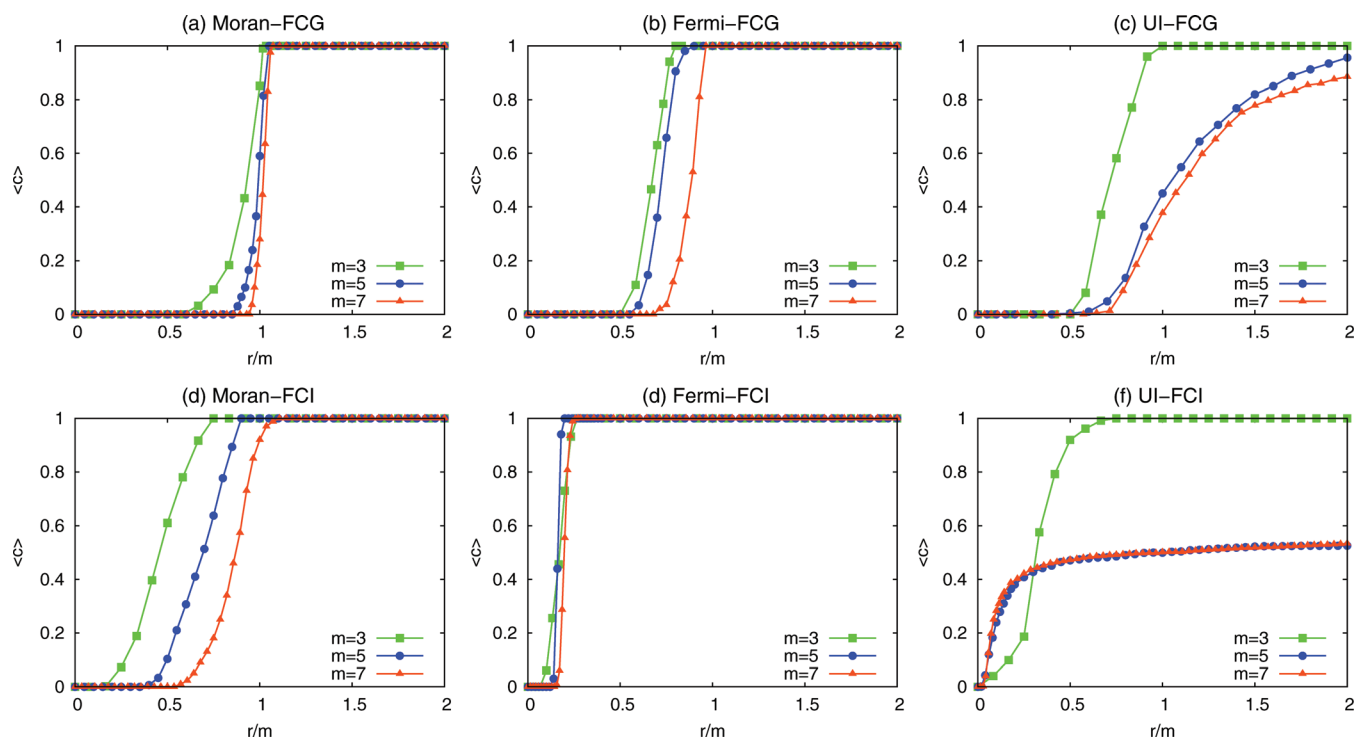


FIG. 5. (Color online) Cooperation level  $\langle c \rangle$  as a function of the rescaled enhancement factor  $r/m$  for the PGG played on top of three synthetic collaboration networks with different group sizes  $m = 3, 5$ , and  $7$ . As in Fig. 4, the first three plots (a), (b), and (c) correspond to the PGG with FCG, while the plots (d), (e), and (f) account for the PGG with FCI. For each of the two versions of the PGG, we show the evolution of the curves  $\langle c \rangle(r/m)$  for three different update rules: (a) and (d) MOR update, (b) and (e) Fermi rule, and (c) and (f) UI.

dynamics, we observe that the dynamics behaves as in the stochastic settings, i.e., the dynamics always ends up into full defection or full cooperation. This convergence, at variance with the stochastic settings, is achieved in few rounds of the PGG, thus pointing out that the dynamical outcome is strongly dependent on the initial conditions. For UI updates, the influence of the most connected players, here represented by those agents participating in a large number of groups, is the key role driving the evolution of the system. Therefore, the existence of large groups enhances both the ubiquity of those players and their benefits. The imitation process provides with an efficient way to spread their initial strategy and trap the system dynamics in one of the two absorbing states. As shown in Fig. 5, for large values of  $r$ , the fraction of realizations in which full cooperation is achieved saturates around 0.5, thus pointing out the strong dependence on the initial strategy of hubs.

## V. CONCLUSIONS

Summarizing our main results, we have shown that is of utmost importance to include the mesoscopic details about the real group structure when dealing with the PGG on networks. The intrinsic group structure (described by means of a bipartite graph) promotes cooperation in PGGs, this being a new mechanism for this phenomenon beyond the scale-free character<sup>21</sup> and other features<sup>39–46</sup> of the one-mode (projected) complex network. Regarding the size of the groups in which the PGG takes place, we have shown that they affect the outcome of the evolutionary dynamics in an important way: In most of the cases, increasing the number of the

participants in each of the groups leads to a decrease of the cooperation level. However, this decrease is influenced by the update rule used. While for MOR and Fermi updates the influence of the size of the groups is quite soft for the case of UI we have shown that large group sizes slow down the development of cooperation due to the large influence of those players participating in a large number of groups.

Our work allows us to draw important conclusions regarding the application of these models and the corresponding research. Thus, looking again at the difference in the behavior observed on the bipartite network and on the projected one, it is clear that the fact that the mean group size in both settings is different plays a role in the promotion of cooperation: Indeed, as is known for PGGs, smaller group sizes require smaller values of  $r$  for cooperation to become a profitable strategy. This obvious fact does not decrease the relevance of our conclusions, because what we are showing is that considering a projected network leads to an overestimating of the amplification factor needed for cooperation, arising from the artificially increased group size. The results in the FCG setting demonstrate that amplification factors between 1 and 2 already lead to cooperation, which are reasonable values in the context we are dealing with, namely collaboration in research and paper-writing. On the other hand, the large value obtained for the MOR rule indicates that this is not likely to be a good model of human behavior in this context, while local imitative rules like Fermi or UI yield lower estimates for the critical  $r$ , probably closer to reality. Note also that we have seen important differences between a setup in which the amount one can invest is unlimited (FCG) or bounded (FCI). This latter scenario,

which is closer to reality in the sense that we all have limited time and energy to devote to collaborative work, gives rise to very low (or even smaller than 1) critical values for  $r$ . This might seem strange at first glance, but when considering this issue on the light of the structure of the bipartite network, one realizes that even with the bipartite description there are authors with a large number of collaborations, i.e., there are hubs. These hubs invest very little on every collaboration they are involved in and in practice become free-riders. However, imitative update rules forces their neighbors to be cooperators as well, because they observe the large payoff received by the hub (arising from his many collaborations), and only under MOR dynamics larger values of  $r$  are needed to support cooperation.

On a different note, our research confirms the intuition that the larger teams are, the more difficult it becomes to foster collaborative work. This is a very relevant insight in so far as it cannot be obtained by looking at the projected network, where the information about group size is lost. Our simulations on a simple model of collaborative network lead to the prediction that, generally speaking, group sizes around  $m=3$  are best to promote cooperation. Note, however, that under Fermi dynamics, the group size is not that important, particularly in the more realistic FCI scenario, for which the critical value of  $r$  appears to be linearly dependent on  $m$ , thus making the group size lose influence. The opposite case arises when UI is used to update strategies, showing that it might be impossible to reach full cooperation even for very large values of  $r$ . It is then clear that accurately modeling the collaboration structure is a key issue when trying to understand why people work together in small groups, with group size and the bipartite character of the network being particularly relevant aspects. Further research is needed to ascertain the way in which individuals update their strategies to complete this incipient modeling toolbox.

## ACKNOWLEDGMENTS

This work has been partially supported by MICINN (Spain) through Grants FIS2008-01240 (J.G.G.), MOSAICO (D.V. and A.S.), and MTM2009-13838 (J.G.G., M.R., and R.C.), and by Comunidad de Madrid (Spain) through Grant MODELICO-CM (A.S.). D.V. acknowledges support from a Postdoctoral Contract from Universidad Carlos III de Madrid. J.G.-G. is supported by the MICINN through the Ramon y Cajal Program.

<sup>1</sup>G. Szabó and G. Fáth, *Phys. Rep.* **446**, 97 (2007).

<sup>2</sup>C. P. Roca, J. Cuesta, and A. Sánchez, *Phys. Life Rev.* **6**, 208 (2009).

<sup>3</sup>M. Newman, *SIAM Rev.* **45**, 167 (2003).

<sup>4</sup>S. Bocaletti, V. Latora, Y. Moreno, M. Chavez, and D. U. Hwang, *Phys. Rep.* **424**, 175 (2006).

<sup>5</sup>M. A. Nowak, *Evolutionary Dynamics: Exploring the Equations of Life* (The Belknap Press of Harvard University, Cambridge, MA, 2006).

<sup>6</sup>M. A. Nowak, *Science* **314**, 1560 (2006).

<sup>7</sup>J. Maynard Smith and E. Szathmáry, *The Major Transitions in Evolution* (Freeman, Oxford, 1995).

<sup>8</sup>*Cooperation in Primates and Humans: Mechanisms and Evolution*, edited by P. M. Kappeler and C. P. van Schaik (Springer-Verlag, Berlin-Heidelberg, 2006).

<sup>9</sup>E. O. Wilson, *Sociobiology* (Belknap Press of Harvard University, 2000), 25th ed.

<sup>10</sup>*Foundations of Human Sociality: Economic Experiments and Ethnographic Evidence from Fifteen Small-Scale Societies*, edited by J. Henrich, R. Boyd, S. Bowles, C. Camerer, E. Fehr, and H. Gintis (Oxford University Press, Oxford, 2004).

<sup>11</sup>A. Rapoport and M. Guyer, *General Systems* **11**, 203 (1966).

<sup>12</sup>R. Axelrod, *The Evolution of Cooperation* (Basic, New York, 1984).

<sup>13</sup>M. W. Macy and A. Flache, *Proc. Natl. Acad. Sci. U.S.A.* **99**, 7229 (2002).

<sup>14</sup>M. A. Nowak and R. M. May, *Nature* **359**, 826 (1992).

<sup>15</sup>C. P. Roca, J. Cuesta, and A. Sánchez, *Phys. Rev. E* **80**, 46106 (2009).

<sup>16</sup>J. H. Kagel and A. E. Roth, *The Handbook of Experimental Economics* (Princeton University, Cambridge, MA, 1995).

<sup>17</sup>G. Hardin, *Science* **162**, 1243 (1968).

<sup>18</sup>H. Brandt, C. Hauert, and K. Sigmund, *Proc. R. Soc. London, Ser. B* **270**, 1099 (2003).

<sup>19</sup>C. Hauert and G. Szabó, *Complexity* **8**, 31 (2003).

<sup>20</sup>A.-L. Barabási and R. Albert, *Science* **286**, 509 (1999).

<sup>21</sup>F. C. Santos, M. D. Santos, and J. M. Pacheco, *Nature* **454**, 213 (2008).

<sup>22</sup>M. Milinski, D. Semmann, H. J. Krambeck, and J. Marotzke, *Proc. Natl. Acad. Sci. U.S.A.* **103**, 3994 (2006).

<sup>23</sup>M. Newman, *Proc. Natl. Acad. Sci. U.S.A.* **98**, 404 (2001).

<sup>24</sup>M. Newman, *Phys. Rev. E* **64**, 016131 (2001).

<sup>25</sup>M. Newman, *Proc. Natl. Acad. Sci. U.S.A.* **101**, 5200 (2004).

<sup>26</sup>S. Lozano, A. Arenas, and A. Sánchez, *PLoS ONE* **3**, e1892 (2008).

<sup>27</sup>S. Lozano, A. Arenas, and A. Sánchez, *J. Econ. Interact. Coord.* **3**, 183 (2008).

<sup>28</sup>S. Assenza, J. Gómez-Gardeñes, and V. Latora, *Phys. Rev. E* **78**, 017101 (2009).

<sup>29</sup>C. P. Roca, S. Lozano, A. Arenas, and A. Sánchez, *PLoS ONE* **5**(12), e15210 (2010).

<sup>30</sup>N. S. Glance and B. A. Huberman, *Sci. Am.* **270**, 76 (1994).

<sup>31</sup>B. A. Huberman and N. S. Glance, *Comp. Econ.* **8**, 27 (1995).

<sup>32</sup>B. A. Huberman and N. S. Glance, in *Modelling Rational and Moral Agents*, edited by P. Danielson (Oxford University Press, Oxford, 1996).

<sup>33</sup>D. Helbing, A. Szolnoki, M. Perc, and G. Szabó, *New J. Phys.* **12**, 083005 (2010).

<sup>34</sup>D. J. Watts and S. H. Strogatz, *Nature* **393**, 440 (1998).

<sup>35</sup>F. C. Santos and J. M. Pacheco, *Phys. Rev. Lett.* **95**, 98104 (2005).

<sup>36</sup>J. Gómez-Gardeñes, M. Campillo, L. M. Floría, and Y. Moreno, *Phys. Rev. Lett.* **98**, 108103 (2007).

<sup>37</sup>J. Poncela, J. Gómez-Gardeñes, L. M. Floría, and Y. Moreno, *J. Theor. Biol.* **253**, 296 (2008).

<sup>38</sup>A. Szolnoki, M. Perc, and G. Szabó, *Phys. Rev. E* **80**, 056109 (2009).

<sup>39</sup>Z.-G. Huang, Z.-X. Wu, A.-C. Wu, L. Yang, and Y.-H. Wang, *EPL* **84**, 50008 (2008).

<sup>40</sup>Z. Rong and Z. X. Wu, *EPL* **87**, 30001 (2009).

<sup>41</sup>D. M. Shi and B. H. Wang, *EPL* **90**, 58003 (2010).

<sup>42</sup>Z. Rong, H.-X. Yang, and W.-X. Wang, *Phys. Rev. E* **82**, 047101 (2010).

<sup>43</sup>D.-M. Shi, H.-X. Yang, M.-B. Hu, W.-B. Du, B.-H. Wang, and X.-B. Cao, *Physica A* **388**, 4646 (2009).

<sup>44</sup>X.-B. Cao, W.-B. Du, and Z.-H. Rong, *Physica A* **389**, 1273 (2010).

<sup>45</sup>D. Peng, H. X. Yang, W. X. Wang, G. R. Chen, and B. H. Wang, *Eur. Phys. J. B* **73**, 455 (2010).

<sup>46</sup>H. Zhang, H. Yang, W. Du, B. Wang, and X. Cao, *Physica A* **389**, 1099 (2010).

<sup>47</sup>J. J. Ramasco, S. N. Dorogovtsev, and R. Pastor-Satorras, *Phys. Rev. E* **70**, 036106 (2004).

<sup>48</sup>R. Guimerà, B. Uzzi, J. Spiro, and L. A. N. Amaral, *Science* **308**, 697 (2005).

<sup>49</sup>M. Peltomäki and M. Alava, *J. Stat. Mech.: Theory Exp.* P01010 (2006).

<sup>50</sup>J. Gómez-Gardeñes, V. Latora, Y. Moreno, and E. Profumo, *Proc. Natl. Acad. Sci. U.S.A.* **105**, 1399 (2008).

<sup>51</sup>G. Szabó and C. Töke, *Phys. Rev. E* **58**, 69 (1998).

<sup>52</sup>A. Traulsen, M. A. Nowak, and J. M. Pacheco, *Phys. Rev. E* **74**, 011909 (2006).

<sup>53</sup>O. Kirchkamp, *J. Econ. Behav. Organ.* **40**, 295 (1999).